Published in final edited form as:
Cancer Discov. 2013 March ; 3(3): 294–307. doi:10.1158/2159-8290.CD-12-0198.

Mutant N-Ras protects colorectal cancer cells from stress-induced apoptosis and contributes to cancer development and progression

Yufang Wang[1], **Sérgia Velho**[1], **Efsevia Vakiani**[2], **Shouyong Peng**[3], **Adam J. Bass**[4], **Gerald C. Chu**[5], **Jessica Gierut**[1], **James M. Bugni**[6], **Channing J. Der**[7], **Mark Philips**[8], **David B. Solit**[9], and **Kevin M. Haigis**[1]

[1]Molecular Pathology Unit, Center for Cancer Research, and Center for Systems Biology, Massachusetts General Hospital, Harvard Medical School, Charlestown, MA 02129

[2]Department of Pathology, Memorial Sloan-Kettering Cancer Center, New York, NY 10021

[3]Department of Medical Oncology and Center for Cancer Genome Discovery, Dana-Farber Cancer Institute, Boston, MA 02115

[4]Department of Medical Oncology and Center for Cancer Genome Discovery, Dana-Farber Cancer Institute, Department of Medicine, Brigham and Women's Hospital, and Department of Medicine, Harvard Medical School, Boston, MA 02115

[5]Department of Medical Oncology, Dana-Farber Cancer Institute, Department of Pathology, Brigham and Women's Hospital, and Department of Medicine, Harvard Medical School, Boston, MA 02115

[6]Inflammatory Bowel Disease Center, Division of Digestive Diseases, David Geffen School of Medicine, University of California at Los Angeles, Los Angeles, CA 90095

[7]Lineberger Comprehensive Cancer Center, Department of Pharmacology, University of North Carolina, Chapel Hill, NC 27599

[8]NYU Cancer Institute, NYU School of Medicine, New York, NY 10016

[9]Department of Medicine, Memorial Sloan-Kettering Cancer Center, 1275 York Avenue, New York, NY 10065

Abstract

N-Ras is one member of a family of oncoproteins that are commonly mutated in cancer. Activating mutations in N-Ras occur in a subset of colorectal cancers, but little in known about how the mutant protein contributes to onset and progression of the disease. Using genetically engineered mice, we find that mutant N-Ras strongly promotes tumorigenesis in the context of inflammation. The pro-tumorigenic nature of mutant N-Ras is related to its anti-apoptotic function, which is mediated by activation of a non-canonical MAPK pathway that signals through Stat3. As a result, inhibition of MEK selectively induces apoptosis in autochthonous colonic tumors expressing mutant N-Ras. The translational significance of this finding is highlighted by our observation that *NRAS* mutation correlates with a less favorable clinical outcome for

Corresponding author: Kevin Haigis, Massachusetts General Hospital, Molecular Pathology Unit, 149 13th Street, 7.372, Charlestown, MA 02129; Phone: 617-643-0070; khaigis@partners.org.
Note: Y. Wang and S. Velho contributed equally to this work.

Conflicts: There are no conflicts of interest to disclose.

colorectal cancer patients. These data demonstrate for the first time the important role that N-Ras plays in colorectal cancer.\

Keywords

Ras; colorectal cancer; MAPK; Stat3

INTRODUCTION

The Ras protein family consists of four highly homologous enzymes (H-Ras, N-Ras, K-Ras4A, and K-Ras4B) that are identical over the first 85 amino acids, 85% identical over the next 80 amino acids, and largely divergent within the C-terminal 24 amino acids, a domain that is referred to as the hypervariable region (HVR). Proteins of the Ras family act as GDP/GTP-regulated switches to mediate cellular responses to extracellular signals (1). When bound to GTP, Ras proteins assume a conformation that allows them to engage and activate a multitude of downstream effectors. Each of the Ras isoforms can be locked into its GTP-bound activated state via missense mutation, typically at amino acid 12, 13, or 61 (2). Mutant Ras proteins accumulate in the GTP-bound conformation due to defective intrinsic GTPase activity and/or resistance to inactivation by GTPase activating proteins (GAPs) (3). Such activating mutations are common in human cancers.

Consistent with the high degree of homology shared by members of the family, biochemical assays have failed to uncover significant differences between Ras isoforms. Nevertheless, genetic studies have revealed apparent isoform-specific phenotypes. In human cancers, for example, mutations in different *RAS* genes are preferentially associated with distinct tumor types. *KRAS* mutations are extremely common in cancers of the pancreas, colon, and lung, while *NRAS* mutations predominate in melanoma and hematopoetic cancers (4). Given the highly conserved enzymatic function of the Ras isoforms, it remains unclear what accounts for their differing mutational frequencies. Whereas variable expression levels and/or patterns in specific tissues might underlie some of the observed biological differences (5), emerging evidence supports the idea that each Ras isoform is truly functionally unique. For example, we reported the generation of mice genetically engineered to express mutationally activated N-Ras (N-Ras^{G12D}) and K-Ras (K-Ras^{G12D}) specifically in the intestinal epithelium (6). While activating mutations in K-Ras occur in 40% of human colorectal cancers (CRCs), N-Ras mutations occur in only 3% (7–9). In the mouse colonic epithelium, K-Ras^{G12D} induces hyper-proliferation that manifests as chronic intestinal hyperplasia and, in the context of mutant Apc, strongly enhances the transition from a benign adenoma to a malignant adenocarcinoma. By contrast, N-Ras^{G12D} does not affect basal homeostasis or tumor progression, but instead inhibits the ability of intestinal epithelial cells to undergo apoptosis in response to stress (6). Presently, it is unclear if/how the anti-apoptotic phenotype associated with mutationally activated N-Ras contributes to the initiation and progression of CRC.

Because N-Ras is the least studied of the Ras family GTPases, its isoform-specific oncogenic properties are not well characterized. Unlike K-Ras and H-Ras, N-Ras is not activated by specific cytokines (e.g. IL-3) or growth factors (e.g. EGF) (10). In myeloma cells, however, expression of mutationally activated N-Ras produces a transcriptional response similar to treatment with IL-6 (11, 12). Although loss of mutant N-Ras in some cell types is associated with a reduction in proliferation (13), N-Ras function has also been linked to the regulation of apoptosis. For example, knockdown of mutant N-Ras in melanoma cells causes apoptosis, suggesting that mutant N-Ras provides a steady state survival signal (14). In our study, we have examined the molecular mechanisms underlying

the anti-apoptotic function of N-Ras in colonic epithelial cells and connected these mechanisms to the ability of mutant N-Ras to promote CRC.

RESULTS

Activated N-Ras Promotes CRC in the Context of Inflammation

We have previously shown that expression of N-Ras^{G12D} in the colonic epithelium has no effect on basal homeostasis, but instead protects the epithelium from apoptosis induced by acute exposure to dextran sodium sulfate (DSS) (6). Based on this observation, we hypothesized that *NRAS* mutations might arise in CRC under circumstances of chronic apoptotic stimulus. Inflammation is a strong risk factor for CRC and it can also promote apoptosis of epithelial cells (15). To determine whether activated N-Ras affects colonic epithelial homeostasis in the context of inflammation, we induced colitis in N-Ras wild-type (*Villin-Cre*, referred to as WT) and N-Ras mutant (*Villin-Cre; Nras*$^{LSL\text{-}G12D}$/+) animals by treating them with cycles of DSS (5 days on, 10 days off). Animals expressing N-Ras^{G12D} were relatively resistant to the chronic effects of DSS, as measured by weight loss and activation of T cells in the mesenteric lymph nodes (Supplementary Fig. S1A–C). And while *Villin-Cre; Nras*$^{LSL\text{-}G12D}$/+ animals developed lower grade inflammation than WT mice, the colonic epithelium was hyperproliferative in N-Ras mutants compared to WT animals (Supplementary Fig. S1D). These observations indicate that expression of mutant N-Ras in the colonic epithelium plays a dual role in this mouse model: (1) it suppresses the initial DSS-induced apoptosis that is required for the initiation of colitis and (2) it promotes hyper-proliferation in the context of colitis.

In WT mice, the extent of colitis typically increases as animals receive sequential cycles of DSS. After 9 cycles of DSS, our WT animals developed severe colitis that was associated with epithelial damage and bleeding ulcers (Fig. 1A,B). The colitis that developed in animals expressing N-Ras^{G12D} was markedly reduced, although focal regions of inflammation were present (Fig. 1A,B). Remarkably, half of the animals expressing N-Ras^{G12D} (but none of the WT controls) developed colonic adenocarcinomas exhibiting high levels of nuclear β-catenin (Fig. 1A,C), suggesting that activated N-Ras promotes CRC driven by inflammation.

An alternative way to induce CRC driven by inflammation is to pre-treat animals with a single dose of the colon-specific carcinogen azoxymethane (AOM), followed by three cycles of DSS (16). Under this protocol, 5/7 WT animals developed colonic tumors, with most animals developing just a single macroscopically visible tumor (Fig. 1D). All of the animals expressing N-Ras^{G12D} (12/12) developed at least a single tumor, with most animals developing multiple (Fig. 1D). Histologically, the tumors expressing mutant N-Ras were not clearly different from those expressing wild-type N-Ras (Fig. 1E, Supplementary Fig. S1E). One explanation for this observation is that AOM/DSS-induced tumors from WT mice acquire N-Ras mutations. To explore this concept, we sequenced exons 2 (containing amino acids 12/13) and 3 (containing amino acid 61) of *Nras* in tumors from WT mice treated with AOM/DSS. We found zero mutations in 21 tumors that were evaluated, indicating that *Nras* is not commonly mutated in AOM/DSS-induced tumors from WT animals.

Since mutant N-Ras enhanced proliferation of the normal epithelium in the context of inflammation, we expected N-Ras mutant tumors to be hyper-proliferative relative to those that developed in a WT background. Unexpectedly, they were not (Supplementary Fig. 1F). Consistent with our previous observation that N-Ras^{G12D} suppresses stress-induced apoptosis, however, we did detect a difference in the basal levels of apoptosis in WT and N-Ras mutant colonic tumors (Fig. 1F). Altogether, these observations suggest that

mutationally activated N-Ras promotes CRC by suppressing the chronic apoptotic stimulus provided by inflammation.

Mutant Forms of Ras Exhibit Unique Apoptotic Phenotypes and Signaling Properties

To uncover the molecular mechanisms underlying the anti-apoptotic function of N-Ras, we generated human colonic epithelial cell lines that differ in their *Ras* genotype. While these cell lines expressed similar levels of Ras (Supplementary Fig. S2), they differed significantly in their ability to enhance proliferation and to suppress apoptosis - only mutant K-Ras induced hyper-proliferation (Supplementary Fig. S3A), while only mutant N-Ras suppressed apoptosis in response to butyrate, a carboxylic acid that induces cell death through both intrinsic and extrinsic apoptotic pathways (Fig. 2A, Supplementary Fig. S3B). These data are consistent with our previous observations that mutant N-Ras alone can function to suppress apoptosis in colonic epithelial cells (6, 17).

Since there are no known human colorectal cancer cell lines expressing mutationally activated N-Ras, our experiments relied on cell lines in which N-Ras^{G12D} was ectopically expressed from a retrovirus. A caveat to these studies is that the anti-apoptotic phenotype associated with mutant N-Ras might be due to over-expression, rather than due to a true functional difference among family members. To address specifically whether the mutant N-Ras in our CRC cell line was over-expressed relative to endogenous mutant N-Ras found in other cancers, we performed Ras activity assays on a panel of cells lines (Supplementary Fig. 4A). This analysis confirmed that the levels of N-Ras•GTP in our CRC cells are comparable to the levels found in cell lines expressing endogenous mutant N-Ras.

Mutant forms of Ras are thought to engage multiple downstream effectors in order to transmit their oncogenic signal. To determine whether mutant N-Ras exhibits unique signaling properties when compared to mutant K-Ras and H-Ras, we used quantitative western blotting to measure the effects of Ras activation on downstream effector pathways in serum-starved cells (Supplementary Fig. S4B). N-Ras^{G12D} activated ERK and AKT (relative to WT), but failed to activate RALA, JNK, or P38 MAPK (Fig. 2B). The signaling properties associated with mutant K-Ras differed somewhat from mutant N-Ras, for example in the activation of AKT, but H-Ras appeared to exhibit identical signaling properties to that of N-Ras (Fig. 2B). Although this signaling analysis did not reveal whether a specific pathway is required for N-Ras function, it did demonstrate that the phenotypic differences between N-Ras and the other family members (*e.g.* H-Ras) cannot be explained by differential signaling through canonical effector pathways.

N-Ras Signals Specifically Through RAF-1 to Suppress Apoptosis

While N-Ras^{G12D} is clearly able to engage multiple downstream pathways, it remained unclear whether activation of a particular effector pathway is necessary or sufficient to mediate its anti-apoptotic phenotype. To address this issue, we generated cell lines expressing N-Ras^{G12D} along with a secondary mutation that restricts signaling to a particular effector pathway (Supplementary Fig. S2) - the T35S mutant binds preferentially to RAF, the E37G mutant shows preference for RALGDS, and the Y40C mutant binds preferentially to PI3K (18). N-Ras$^{G12D/T35S}$ fully phenocopied N-Ras^{G12D} with respect to its ability to confer resistance to butryate-induced apoptosis (Fig. 2C). This observation indicates that binding to RAF is *sufficient* for mutant N-Ras to protect cells from apoptosis. To confirm this result, we pretreated cells with AZ-628, a pan-RAF inhibitor, prior to induction of apoptosis with sodium butyrate. Inhibition of RAF had no effect on the apoptotic phenotype of WT cells, but reversed the anti-apoptotic phenotype of N-Ras^{G12D} (Fig. 2D), indicating that RAF signaling is required downstream of N-RAS.

RAF is a protein family that consists of three highly related serine/threonine kinases, A-RAF, B-RAF, and C-RAF (also called RAF-1). To determine whether one RAF family member mediates the N-Ras anti-apoptotic phenotype, we used lentivirus-mediated shRNA to knock down RAF levels in cells expressing wild-type or mutant N-Ras (Supplementary Fig. S5A). Knockdown of RAF-1, but not A-RAF or B-RAF, reverted the N-Ras phenotype toward that of WT (Fig. 2E, Supplementary Fig. S5B), suggesting that RAF-1, in particular, mediates the anti-apoptotic function of N-Ras^{G12D}. To explore this concept further, we expressed different activated forms of RAF in CRC cells that were wild-type for N-RAS. Expression of mutationally activated RAF-1 protected cells from butyrate-induced apoptosis to the same extent as activated N-Ras (Fig. 2F). Expression of B-RAF or A-RAF did not phenocopy N-Ras, even though all three forms of RAF could activate ERK to the same extent (Fig. 2F,G).

Altogether, our data have demonstrated that N-Ras alone suppressed butyrate-induced apoptosis, even though all of the Ras family members could activate ERK (Fig. 2B). Moreover, we found that RAF-1 was also unique within the RAF kinase family in its ability to suppress apoptosis, while all of the RAF family members activated ERK to roughly the same extent (Fig. 2G). Based on these observations, we considered the possibility that (1) a MEK/ERK-independent pathway functions cooperatively downstream of N-Ras/RAF-1 to suppress butryate-induced apoptosis or (2) a non-canonical MAPK pathways was mediating the anti-apoptotic function of mutant N-Ras.

N-Ras Mediates IL-6→Stat3 Signaling

Mutationally activated N-Ras can confer cytokine-independent growth upon previously IL-6-dependent cell lines (11, 12). Studies of mouse models have also demonstrated that IL-6 signaling also plays an important role in inflammation-driven CRC (19, 20). By extension, we explored whether N-Ras actively functions within the IL-6 signaling pathway to control the response of CRC cells to apoptotic stimuli. To begin, we treated WT and mutant cells with exogenous IL-6. When exposed to IL-6, cells expressing wild-type N-Ras became partially resistant to butyrate-induced apoptosis (Fig. 3A). IL-6 treatment failed to further protect cells expressing mutant N-Ras, suggesting that the downstream pathway activated by IL-6 was already activated in cells expressing N-Ras^{G12D} (Fig. 3A).

The primary downstream effector of IL-6R function is the Stat3 transcription factor (21). Cells expressing N-Ras^{G12D} or RAF-1$^{Y340/341D}$ expressed two-fold higher levels of Stat3 phosphorylated on Tyr705 than did cells expressing wild-type Ras or mutant forms of K-Ras and H-Ras (Fig. 3B). Surprisingly, although ERK was highly activated in cells expressing mutant N-Ras, there was no change in the phosphorylation state of Ser727, an ERK phosphorylation site (Supplementary Fig. S6A). Stat3 is a transcription factor that regulates the expression of genes involved in proliferation and survival (21). We found that CRC cells expressing mutant N-Ras expressed higher levels of the canonical Stat3 target genes *CCND1* and *SOCS3* relative to WT (Fig. 3C). Similarly, we found that genes negatively regulated by Stat3 (*IFIT3* and *IFI35*) were expressed at lower levels in cells expressing N-Ras^{G12D} (Fig. 3C).

We next analyzed the apoptotic phenotypes of WT and mutant cells that lack Stat3. Similar to loss of RAF-1, loss of Stat3 reverted the N-Ras phenotype, but had no significant effect on the butyrate response of WT cells (Fig. 3D). We also found that a small molecule inhibitor of Stat3 (Stattic) could also revert the apoptotic phenotype of N-Ras mutant cells to WT (Fig. 3E). Taken together, our results indicate that mutant N-Ras signals through Stat3 to regulate the cellular response to butyrate.

Our data suggested that N-Ras^{G12D} suppresses apoptosis by activating RAF-1 and Stat3, but it was unclear whether these signals were dependent or independent of one another. To explore this question, we examined the phosphorylation status of Stat3 in cells that were treated with CI-1040, a MEK inhibitor (22). MEK is the only *bona fide* effector of RAF signaling. Inhibition of MEK led to a decrease in the phosphorylation status of Stat3 in cells expressing N-Ras^{G12D} (Fig. 3F). Alternatively, shRNA-mediated knockdown of Stat3 had no effect on the activation state of ERK (Supplementary Fig. S6B). These data suggest that N-Ras^{G12D} activates Stat3 downstream of MEK.

N-RAS•GTP Forms a Complex with RAF-1 and Stat3

How does N-Ras activate Stat3 and why is it the only family member that can do so? One possibility is that mutant N-Ras induces an autocrine IL-6 feedback loop that activates Stat3 downstream of IL-6R. Contrary to this hypothesis, we did not detect an increase in secreted IL-6 in the culture media of cells expressing N-Ras^{G12D} (Supplementary Fig. S6C). Moreover, conditioned medium from cells expressing mutant N-Ras was not able to activate Stat3 in WT cells (Supplementary Fig. S6D). Based on these data, we believed that it was more likely that mutant N-Ras was directly activating Stat3 by forming a complex with it. Indeed, we found that N-Ras^{G12D}, but not K-Ras^{G13D} nor H-Ras^{G12V}, co-immunoprecipitated with Stat3 (Fig. 3G, Supplementary Fig. S6E,F). Consistent with our observation that mutant RAF-1 also activated Stat3, RAF-1 immunoprecipitated with Stat3 (Supplementary Fig. S6G). These results indicate that activated N-Ras forms an anti-apoptotic signaling complex that includes Stat3 and RAF-1.

Mutant N-Ras Signals From Cholesterol-rich Microdomains to Suppress Apoptosis

Mutant forms of N-Ras and H-Ras are equal in their ability to activate ERK, but only N-Ras can activate Stat3. We hypothesized that their differing abilities to activate Stat3 may result from a difference in sub-cellular localization. Consistent with this hypothesis, replacing the H-Ras HVR with that of N-Ras allowed H-Ras to suppress butyrate-induced apoptosis, suggesting that the anti-apoptotic phenotype of mutant N-Ras is specified by its localization (Fig. 4A). On the plasma membrane, GTP-bound forms of N-Ras and H-Ras are thought to differ in their distributions among cholesterol-rich microdomains (23, 24). Following biochemical purification, we found that mutant N-Ras, but not mutant H-Ras, could be detected in caveolin-rich fractions (Fig. 4B). Consistent with our proposed mechanism of action of mutant N-Ras, we found that ERK and Stat3 were highly enriched in the same fractions as N-Ras (Fig. 4B). Caveolae can be dissociated by exposure to filipin, an antifungal agent isolated from *Streptomyces filipensis*, or to methyl-β-cyclodextrin (MβCD). The ability of N-Ras to co-immunoprecipitate with Stat3 was affected by treatment of cells with filipin (Fig. 3G) and transient exposure to filipin or MβCD abrogated the anti-apoptotic phenotype of mutant N-Ras (Fig. 4C), suggesting that, in CRC cells, N-Ras signals from caveolae to suppress apoptosis.

Mutant N-Ras activates ERK and Stat3 in Primary Cancers

To determine whether mutant N-Ras signals through ERK and Stat3 in primary CRCs, we examined their activation states in tumors from mice and humans by immunohistochemistry. In tumors from AOM/DSS treated animals, there was no detectable difference in ERK activation between WT and N-Ras mutant tumors, primarily because ERK was strongly activated in all tumors (Fig. 5A,B). In human samples, however, CRCs expressing mutant forms of N-Ras exhibited a dramatic enhancement of phospho-ERK staining (Fig. 5A,B). To expand upon this observation, we used gene set enrichment analysis (GSEA) to measure differences in gene expression between primary human CRCs that were wild-type or mutant for N-Ras. Consistent with our IHC analysis, we found that the expression of genes related

to MAPK signaling was significantly enriched in cancers expressing mutant N-Ras relative to those that were wild-type (Fig. 5C).

In both mouse and human tumors, we found that mutant N-Ras strongly activated Stat3 (Fig. 5D,E). GSEA analysis failed to identify enrichment within N-Ras mutant cancers for genes that are up-regulated by Stat3 (data not shown). Interestingly, however, genes known to be negatively regulated by Stat3 were significantly under expressed in cancers expressing mutant N-Ras (Fig. 5F), indicating that Stat3 transcriptional activity is enhanced in the context of N-Ras mutation. These results are consistent with the notion that mutant N-Ras activates the non-canonical MAPK/Stat3 signaling in primary CRC and raises the possibility that therapeutically targeting this pathway could be an effective way to treat N-Ras mutant cancer.

A Therapeutic Strategy for CRCs Expressing Mutant N-Ras

What is the most effective way to target the MAPK pathway therapeutically? Over the past several years, a hanful of highly specific MEK inhibitors have entered the lab and clinic (22, 25–27). Given that we had already shown that inhibition of MEK with CI-1040 could abrogate the activation of Stat3 downstream of N-Ras^{G12D} (Fig. 3F), we next tested whether it could revert the anti-apoptotic phenotype associated with mutant N-Ras. As with pharmacologic inhibition of RAF, inhibition of MEK suppressed the N-Ras apoptosis phenotype (Fig. 6A). Next, we treated mice bearing AOM/DSS-induced tumors with CI-1040. Acute inhibition of MEK induced apoptosis in tumors expressing N-Ras^{G12D}, but not in WT tumors (Fig. 6B). Together, these data suggest that MEK inhibitors could be highly efficacious for patients with N-Ras mutant CRC.

One major question that remains is: How significant is mutationally activated N-Ras to CRC in human patients? To address this question, we determined the *NRAS* mutational status of 581 CRCs from patients treated at Memorial Sloan Kettering Cancer Center. Consistent with previous reports (8, 9), we found activating mutations in *NRAS* in approximately 3% of cases (17/581) (Supplementary Table S1). Importantly, when compared with patients whose cancers were WT for *NRAS*, *KRAS*, and *BRAF*, patients with *NRAS* mutant cancers experienced significantly worse overall survival, similar to those with mutations in *KRAS* (Fig. 6C). This observation highlights the importance of identifying new therapies, for example MEK inhibition, for CRCs expressing mutant N-Ras.

DISCUSSION

CRC is a paradigm for the cooperative action of mutations in oncogenes and tumor suppressor genes (28). Understanding the disease at a level that will allow for *a priori* prediction of viable therapeutic targets will require a mechanistic elucidation of each of the mutational events that contribute to initiation and progression. Of particular importance is whether specific mutational events are cooperative or redundant, or whether they may contribute to the development of distinct subtypes of CRC. For example, based on mutational analysis of CRC, mutations in *KRAS* and *NRAS* appear to be redundant, as they are not typically found in the same tumor (Supplementary Table S1) (8, 9). As a result, one might predict that a common therapeutic strategy would work for cancers that carry mutations in either of these two genes. Yet our functional analysis demonstrated that mice expressing mutationally activated forms of K-Ras or N-Ras in the colonic epithelium exhibited essentially non-overlapping phenotypes (6). We interpret these observations to mean that *KRAS* and *NRAS* mutations are mutually exclusive, not because they are redundant, because they are selected for under distinct tumorigenic contexts. The differential apoptotic function of N-Ras and K-Ras led us to speculate that *NRAS* mutations might arise specifically under circumstances of chronic apoptotic stimulus. Indeed, our studies of

genetically engineered mice indicated that N-Ras^{G12D} enhances colon cancer development in the context of inflammation (Fig. 1). Both chronic, for example in inflammatory bowel disease (IBD), and acute inflammation contribute to the progression of CRC (29).

Using both *in vitro* and *in vivo* systems, we sought to uncover the molecular mechanisms that underlie the unique anti-apoptotic function of N-Ras. In other cell types, mutant N-Ras has been correlatively linked to numerous survival and apoptotic pathways, including BCL2, AKT, JNK, and p38 (30–33). Our data fail to implicate these previously identified pathways in mediating N-Ras function in colonic epithelial cells, suggesting that the pathways utilized by mutant N-Ras to suppress apoptosis are context dependent. Our data indicated that N-Ras^{G12D} requires only RAF-1 to suppress apoptosis (Fig. 2C–E). While each Ras family member is believed to bind all of the RAF family members, the specific engagement of RAF-1 by mutant N-Ras has also been observed in melanoma cells (34). Although N-Ras signals through RAF-1 to activate the canonical MAPK pathway, the RAF-dependent activation of ERK was not sufficient to explain the anti-apoptotic phenotype associated with mutant N-Ras, however. Based on previous reports of N-Ras function in myeloma cells (11, 12), we examined whether Stat3 plays a role in the anti-apoptotic function of N-Ras and RAF-1. Indeed, cells expressing mutant N-Ras exhibit hyper-phosphorylation of Stat3 on Tyr705 and Stat3 was required for the anti-apoptotic function of N-Ras^{G12D} (Fig. 3). Interestingly, Stat3 was also activated by endogenous mutant N-Ras when it was expressed in hematopoetic cells, suggesting that the non-canonical MAPK pathway may be functioning in other contexts as well (35).

Since Stat3 functions as a transcription factor, we confirmed that it was functionally activated by measuring the expression levels of known Stat3 targets in cell lines and primary cancers expressing mutant N-Ras (Fig. 3C,5F). Gene set enrichment analysis (GSEA) of mRNA expression data from human CRCs failed to identify enrichment for genes that are up-regulated by Stat3 in cancers expressing mutant N-Ras. By contrast, GSEA identified a significant negative enrichment for genes that are down-regulated by Stat3 in cancers expressing mutant N-Ras (Fig. 5F). While it is somewhat difficult to interpret a lack of correlation in GSEA (i.e. the failure to find significant over-expression of Stat3 targets), this observation suggests that mutant N-Ras may specifically regulate the transcriptional repressive function of Stat3. While Stat3 is primarily known as a transcriptional activator, and many of its targets (e.g. CyclinD1) are thought to promote cancer, it can also associate with the Kap1 co-repressor to inhibit gene expression (36). The breadth and biological significance of the genes that are negatively regulated by Stat3 are not clear, but they may play an important role in the anti-apoptotic function of mutationally activated N-Ras.

Our finding that N-Ras is unique among the Ras family members in its ability to bind Stat3 is not surprising, as other Ras family members also have unique binding partners. Galectins, for example, are a family of proteins that are characterized by their ability to bind β-galactoside. Mutant H-Ras binds galectin-1 more efficiently than does mutant K-Ras and this interaction stimulates RAF activation at the expense of PI3K activation (37). Conversely, activated K-Ras binds more efficiently to galectin-3, resulting in prolonged activation of RAF and attenuation of PI3K and RAL signaling (38, 39). We speculate that isoform-specific downstream effectors account, at least in part, for the functional differences among Ras family members.

Why is N-Ras the only family member that can interact with and activate Stat3? Each Ras family member is subjected to a different pattern of and palmitoylation within its hypervariable region (40). These post-translational modifications affect the trafficking of Ras family members through the cell, as well as their overall steady-state localization. Within membranes, Ras family members have been found to localize to distinct

microdomains in a manner that is dependent upon their nucleotide binding state. N-Ras•GTP, for example, was found in cholesterol-rich lipid rafts, while H-Ras•GTP localized to disordered membrane (23, 24). In our study, we failed to detect N-Ras in LYN-positive lipid raft fractions in CRC cells, but we did find that N-Ras and H-Ras purified in distinct membrane fractions (Fig. 4B). Moreover, disruption of cholesterol-rich microdomains via treatment with filipin or MβCD abrogates resistance to apoptosis in cells expressing N-Ras^{G12D} (Fig. 4C), indicating that microdomain localization is a major determinant underlying the unique anti-apoptotic phenotype of mutant N-Ras. As such, this subtle feature of Ras localization becomes of central importance to the oncogenic function of this protein.

Our studies clearly establish that N-Ras, unlike K-Ras and H-Ras, can suppress stress-induced apoptosis because it activates a non-canonical MAPK pathway. A major question resulting from this observation is whether this mechanism can be taken advantage of as a therapeutic strategy. In human cell lines, pharmacologic inhibition of MEK abrogated the anti-apoptotic function of mutant N-Ras (Fig. 6A). Two recent studies of large human cell line panels also connected N-Ras mutation to sensitivity to MEK inhibitors (41, 42). We also found that inhibition of MEK induced apoptosis in primary mouse tumors expressing mutant N-Ras (Fig. 6B), providing a critical *in vivo* validation of the *in vitro* results. These observations suggest that MEK inhibitors may be useful in the clinic to treatment patients with N-Ras mutant CRC. This result is especially significant because, as we have demonstrated previously, CRCs expressing mutant K-Ras are not sensitive to MEK inhibition (6).

Taken together, these experiments connect the anti-apoptotic function of mutationally activated N-Ras to its oncogenic potential. Moreover, while we have demonstrated that mutation of N-Ras affects the survival of CRC patients, our biochemical data suggest a viable therapeutic strategy – inhibition of MAPK signaling – for these patients.

METHODS

Human Studies

Clinical data were collected on patients under protocols approved by the Institutional Review Boards of MSKCC and the MGH. Tumor associated mutations were identified as previously described (9). Gene set enrichment analysis (GSEA) was performed as described (43) on published RNAseq data from The Cancer Genome Atlas (TCGA) (44). Individual samples were separated based on their *KRAS*, *NRAS*, and *BRAF* genotypes. The gene set corresponding to 39 targets down-regulated by Stat3 was manually collated from (45).

Induction of Colitis and Cancer in Mice

All experiments involving animals were approved by the MGH Subcommittee on Research Animal Care. Animals expressing K-Ras^{G12D} and N-Ras^{G12D} in the intestinal epithelium were previously described (6). Intestine-specific activation of Ras was achieved by crossing to *Villin-Cre*, which directs expression of Cre recombinase to all crypts of the small intestinal and colonic epithelia (46). Eight-week-old mice were used in all experiments.

To stimulate colitis, mice were treated with 5 or 9 cycles of 2.5% DSS in the drinking water (5 days on, followed by 10 days off). Mice were weighed on a daily basis and colonoscopy was performed to monitor disease progression. At the end of the treatment, mice were sacrificed and tumor number was assessed by macroscopic examination of the dissected colon. The tissue was then fixed overnight in 10% formalin and processed for histologic analyses.

In the AOM/DSS model of inflammation-induced colon cancer, animals were treated with a single injection of azoxymethane (AOM, 10 mg/kg) on the first day and were then exposed to 3 cycles of 2.5% DSS (7 days on, 14 days off). Body weight was monitored daily. Five weeks after ending the treatment period, animals were sacrificed. Tumor number was scored by macroscopic examination of the dissected colon. The tissue was then fixed overnight in 10% formalin and processed for histologic analyses.

Mouse Colonoscopy

On the day before colonoscopy, animals were fasted for 18–24 hours during which time they were given NuLYTELY, a bowel-cleansing solution of polyethylene glycol. Prior to the procedure, animals were anesthetized with Avertin (250 mg/kg). After sedation, the colon was flushed with phosphate buffered saline (PBS) to remove any remaining fecal debris. Colonoscopy was performed using a veterinary endoscope from Karl Storz Endoscopy.

CI-1040 Treatment of Mice

CI-1040 was obtained from Pfizer. N-Ras mutant and WT mice were submitted to AOM/DSS treatment to induce tumor formation. Tumor development was monitored by colonoscopy and only those mice harboring tumors were selected for CI-1040 treatment. These mice were treated with two doses/day of 100 mg/kg of CI-1040 for 7 days. At the end of the treatment, tumors were excised and snap frozen to extract protein for western blot analyses. The levels of apoptosis were examined by quantitative western blotting using an antibody against cleaved-caspase 3.

Immunohistochemistry

Immunohistochemistry was performed on sections (5 μM) of paraffin embedded mouse and human tissues. Antibodies for phospho-Histone H3 (PH3, Ser10), phospho-ERK (Thr202/Tyr204), and phospho-Stat3 (Tyr705) were from Cell Signaling Technologies. The monoclonal antibody against CTNNB1 was from BD Biosciences. Immunohistochemistry was performed following manufacturers instructions for each antibody. Proliferative indices were quantified via PH3 immunohistochemistry. The proliferative index of the normal epithelium was determined by counting the number of PH3-positive cells per crypt. To achieve statistical significance, at least 50 crypts were counted per sample. The proliferative index of tumors was assessed by counting the percentage of PH3-positive epithelial cells. Several magnification fields were analyzed to account for intra-tumoral variability.

For phospho-ERK, both human and mouse tumors were classified in accordance with the intensity of the staining as well as the relative number of positive tumor glands. Phospho-Stat3 scoring was only based on the intensity of the staining, since its expression was relatively homogeneous throughout the tumors.

Cell Culture, Infections, and Apoptotic Assays

DLD-1, DKs-8, HCT-116, and HKe-3 human colorectal cancer cells have been described (47) and were provided to us by Dr. Robert Coffey (Vanderbilt University). Their identities were confirmed by RBD pulldown analysis (Supplementary Fig. 2). Melanoma cell lines were provided by Dr. Lawrence Kwong (Dana Farber Cancer Institute). They were not verified.

The pBabe retrovirus system was used to generate DKs-8 and HKe-3 cells expressing mutant forms of Ras. The DKs-8 and DBN isogenic pair was used for all experiments, except for those described in Supplementary Fig. S3B. Gene knockdown was achieved with pSICOR lentiviral shRNAs (48). To analyze apoptotic responses and cell signaling, cells were plated at 80% confluence with complete medium for 24 h and then incubated in

medium without serum for 12 h. followed by treatment with sodium butyrate for the indicated timeframes. Apoptotic cells were quantified using the FITC-Annexin V Apoptosis Detection Kit I according to manufacturer's instructions (BD Biosciences). Each experiment was performed at least twice, with each independent trial including biological triplicates. All statistical analyses were performed by Wilcoxon Rank Sum test using the MStat computer program.

Real time PCR

The mRNA expression levels of Stat3 targets were measured by real time PCR. RNA was extracted using the RNeasy mini kit (Qiagen). cDNA was synthesize using 2 μg of pure RNA using SuperScript III Reverse transcriptase kit (Invitrogen). One μl of cDNA (diluted 1:5) was added to a 20 μl real time PCR mixture containing 1X TaqMan Universal PCR Master Mix, No AmpErase UNG, and 1x TaqMan MGB specific probes. TaqMan expression assays were purchased from Applied Biosystems. Standard TaqMan thermocycling conditions were employed. Real time PCR assays were performed on three biological replicates.

Expression Vectors

pBabe(puro)-H-Ras^{G12V} and pBabe(puro)RAF1-Y340/341D have been described previously (49). pBabe(puro)-N-Ras^{G12D}, pBabe(puro)-N-Ras^{G12D}-H-HVR, pBabe(puro)-H-Ras^{G12V}-N-HVR, pBabe(puro)-RAF1-22W, pBabe(puro)-B-RAF, and pBabe(puro)-A-RAF-Y304/305D were generated for this study. The Ras effector loop domain mutants T35S, E37G, and Y40C were generated in pBabe-N-Ras^{G12D} by site-directed mutagenesis. shRNAs for N-Ras, Stat3, A-RAF, B-RAF, and RAF-1 were designed with pSICOoligomaker and then cloned into pSicoR (48). Target sequences for specific shRNAs are listed in Supplementary Table S2.

Membrane Fractionations

Cellular fractionation was carried out using the simplified method for the preparation of detergent-free lipid rafts described by Macdonald and Pike (50). Briefly, cells were seeded in 150mm dishes at similar densities. When the cells were approximately 90% confluent, protein was extracted following the protocol described by Macdonald et al. Fifty μl of each fraction were used to analyze the distribution of N-Ras, H-Ras, ERK, Stat3, Caveolin 1, LYN, and Transferrin receptor by quantitative western blotting.

Drug Treatments

AZ-628 was obtained from AstraZeneca. Cells were pre-treated with AZ-628 (1 μM) for one hour prior to treatment with butyrate or isolation of protein. Filipin and MβCD were purchased from Sigma. In specified experiments, cells were transiently treated with filipin (1 μg/ml) or MβCD (10 mM) for 2 hours, at which point the medium was replaced with serum-free medium +/− sodium butyrate (3 mM).

Immunoblotting and GTPase Activity Assays

For western blotting, protein lysates were harvested with RIPA buffer. Quantitative western blots were performed using the LiCor Odyssey. Antibodies to the following proteins were used: ERK1/2, phospho-ERK1/2 (Thr202/Tyr204, Thr185/Tyr187), AKT, phospho-AKT (Ser473), JNK, phospho-JNK (Thr183/Tyr185), p38 MAPK, phospho-p38 MAPK (Thr180/Tyr182), Stat3, and phospho-Stat3 (Tyr705 or Ser727) from Cell Signaling Technology. Additional antibodies included, β-tubulin from Sigma and N-Ras, H-Ras, K-Ras, A-RAF, B-RAF, and RAF-1 from Santa Cruz Biotechnology. Secondary antibodies were from LiCor. Ras and RAL activities were assessed with assay kits from Millipore. For N-Ras activity, N-

Ras-specific antibody was used. For RAL, the RALA antibody included with the kit was used.

Immunoprecipitations

For immunoprecipitations, protein lysates were collected in 1X cell lysis buffer (Cell Signaling Technology). Immobilized Stat3 (79D7) rabbit antibody was used to purify Stat3 complexes from lysates. For immunoprecipitation of N-Ras, a mouse monoclonal antibody was used (Santa Cruz Biotechnology).

Supplementary Material

Refer to Web version on PubMed Central for supplementary material.

Acknowledgments

S.V. is supported by a postdoctoral fellowship from the Portuguese Fundação para a Ciência e a Tecnologia. K.H. was supported by a grant from the National Cancer Institute (CA118425) and by a Pilot Feasibility Award from the MGH Center for the Study of IBD (DK043351). We thank Lawrence Kwong for the gift of the N-Ras mutant melanoma cell lines.

Abbreviations

AOM	azoxymethane
CRC	colorectal cancer
DSS	dextran sodium sulfate
GAP	GTPase activating protein
GSEA	gene set enrichment analysis
HVR	hypervariable region
MAPK	mitogen activated protein kinase
MβCD	methyl-β-cyclodextrin
WT	wild-type

References

1. Malumbres M, Barbacid M. RAS oncogenes: the first 30 years. Nat Rev Cancer. 2003; 3:459–65. [PubMed: 12778136]
2. Campbell SL, Khosravi-Far R, Rossman KL, Clark GJ, Der CJ. Increasing complexity of Ras signaling. Oncogene. 1998; 17:1395–413. [PubMed: 9779987]
3. Donovan S, Shannon KM, Bollag G. GTPase activating proteins: critical regulators of intracellular signaling. Biochim Biophys Acta. 2002; 1602:23–45. [PubMed: 11960693]
4. Lau KS, Haigis KM. Non-redundancy within the RAS oncogene family: Insights into mutational disparities in cancer. Mol Cells. 2009; 28:315–20. [PubMed: 19812895]
5. To MD, Wong CE, Karnezis AN, Del Rosario R, Di Lauro R, Balmain A. Kras regulatory elements and exon 4A determine mutation specificity in lung cancer. Nat Genet. 2008; 40:1240–4. [PubMed: 18758463]
6. Haigis KM, Kendall KR, Wang Y, Cheung A, Haigis MC, Glickman JN, et al. Differential effects of oncogenic K-Ras and N-Ras on proliferation, differentiation and tumor progression in the colon. Nat Genet. 2008; 40:600–8. [PubMed: 18372904]

7. Vogelstein B, Fearon ER, Hamilton SR, Kern SE, Preisinger AC, Leppert M, et al. Genetic alterations during colorectal-tumor development. New Engl J Med. 1988; 319:525–32. [PubMed: 2841597]
8. Irahara N, Baba Y, Nosho K, Shima K, Yan L, Dias-Santagata D, et al. NRAS mutations are rare in colorectal cancer. Diagn Mol Pathol. 2010; 19:157–63. [PubMed: 20736745]
9. Janakiraman M, Vakiani E, Zeng Z, Pratilas CA, Taylor BS, Chitale D, et al. Genomic and biological characterization of exon 4 KRAS mutations in human cancer. Cancer Res. 2010; 70:5901–11. [PubMed: 20570890]
10. Ehrhardt A, David MD, Ehrhardt GR, Schrader JW. Distinct mechanisms determine the patterns of differential activation of H-Ras, N-Ras, K-Ras 4B, and M-Ras by receptors for growth factors or antigen. Mol Cell Biol. 2004; 24:6311–23. [PubMed: 15226433]
11. Croonquist PA, Linden MA, Zhao F, Van Ness BG. Gene profiling of a myeloma cell line reveals similarities and unique signatures among IL-6 response, N-ras-activating mutations, and coculture with bone marrow stromal cells. Blood. 2003; 102:2581–92. [PubMed: 12791645]
12. Hu L, Shi Y, Hsu JH, Gera J, Van Ness B, Lichtenstein A. Downstream effectors of oncogenic ras in multiple myeloma cells. Blood. 2003; 101:3126–35. [PubMed: 12515720]
13. Plattner R, Gupta S, Khosravi-Far R, Sato KY, Perucho M, Der CJ, et al. Differential contribution of the ERK and JNK mitogen-activated protein kinase cascades to Ras transformation of HT1080 fibrosarcoma and DLD-1 colon carcinoma cells. Oncogene. 1999; 18:1807–17. [PubMed: 10086335]
14. Eskandarpour M, Kiaii S, Zhu C, Castro J, Sakko AJ, Hansson J. Suppression of oncogenic NRAS by RNA interference induces apoptosis of human melanoma cells. Int J Cancer. 2005; 115:65–73. [PubMed: 15688405]
15. Eaden JA, Mayberry JF. Colorectal cancer complicating ulcerative colitis: a review. Am J Gastroenterol. 2000; 95:2710–9. [PubMed: 11051339]
16. Neufert C, Becker C, Neurath MF. An inducible mouse model of colon carcinogenesis for the analysis of sporadic and inflammation-driven tumor progression. Nat Prot. 2007; 2:1998–2004.
17. Keller JW, Haigis KM, Franklin JL, Whitehead RH, Jacks T, Coffey RJ. Oncogenic K-RAS subverts the antiapoptotic role of N-RAS and alters modulation of the N-RAS:gelsolin complex. Oncogene. 2007; 26:3051–9. [PubMed: 17130841]
18. White MA, Nicolette C, Minden A, Polverino A, Van Aelst L, Karin M, et al. Multiple Ras functions can contribute to mammalian cell transformation. Cell. 1995; 80:533–41. [PubMed: 7867061]
19. Grivennikov S, Karin E, Terzic J, Mucida D, Yu GY, Vallabhapurapu S, et al. IL-6 and Stat3 are required for survival of intestinal epithelial cells and development of colitis-associated cancer. Cancer Cell. 2009; 15:103–13. [PubMed: 19185845]
20. Bollrath J, Phesse TJ, von Burstin VA, Putoczki T, Bennecke M, Bateman T, et al. gp130-mediated Stat3 activation in enterocytes regulates cell survival and cell-cycle progression during colitis-associated tumorigenesis. Cancer Cell. 2009; 15:91–102. [PubMed: 19185844]
21. Yu H, Pardoll D, Jove R. STATs in cancer inflammation and immunity: a leading role for STAT3. Nat Rev Cancer. 2009; 9:798–809. [PubMed: 19851315]
22. Rinehart J, Adjei AA, Lorusso PM, Waterhouse D, Hecht JR, Natale RB, et al. Multicenter phase II study of the oral MEK inhibitor, CI-1040, in patients with advanced non-small-cell lung, breast, colon, and pancreatic cancer. J Clin Oncol. 2004; 22:4456–62. [PubMed: 15483017]
23. Roy S, Plowman S, Rotblat B, Prior IA, Muncke C, Grainger S, et al. Individual palmitoyl residues serve distinct roles in H-ras trafficking, microlocalization, and signaling. Mol Cell Biol. 2005; 25:6722–33. [PubMed: 16024806]
24. Prior IA, Muncke C, Parton RG, Hancock JF. Direct visualization of Ras proteins in spatially distinct cell surface microdomains. J Cell Biol. 2003; 160:165–70. [PubMed: 12527752]
25. LoRusso PM, Krishnamurthi SS, Rinehart JJ, Nabell LM, Malburg L, Chapman PB, et al. Phase I pharmacokinetic and pharmacodynamic study of the oral MAPK/ERK kinase inhibitor PD-0325901 in patients with advanced cancers. Clin Cancer Res. 2010; 16:1924–37. [PubMed: 20215549]

26. Adjei AA, Cohen RB, Franklin W, Morris C, Wilson D, Molina JR, et al. Phase I pharmacokinetic and pharmacodynamic study of the oral, small-molecule mitogen-activated protein kinase kinase 1/2 inhibitor AZD6244 (ARRY-142886) in patients with advanced cancers. J Clin Oncol. 2008; 26:2139–46. [PubMed: 18390968]
27. Gilmartin AG, Bleam MR, Groy A, Moss KG, Minthorn EA, Kulkarni SG, et al. GSK1120212 (JTP-74057) is an inhibitor of MEK activity and activation with favorable pharmacokinetic properties for sustained in vivo pathway inhibition. Clin Cancer Res. 2011; 17:989–1000. [PubMed: 21245089]
28. Fearon ER, Vogelstein B. A genetic model for colorectal tumorigenesis. Cell. 1990; 61:759–67. [PubMed: 2188735]
29. Terzic J, Grivennikov S, Karin E, Karin M. Inflammation and colon cancer. Gastroenterology. 2010; 138:2101–14. e5. [PubMed: 20420949]
30. Borner C, Schlagbauer Wadl H, Fellay I, Selzer E, Polterauer P, Jansen B. Mutated N-ras upregulates Bcl-2 in human melanoma in vitro and in SCID mice. Melanoma Res. 1999; 9:347–50. [PubMed: 10504052]
31. Urquhart JL, Meech SJ, Marr DG, Shellman YG, Duke RC, Norris DA. Regulation of Fas-mediated apoptosis by N-ras in melanoma. J Invest Dermatol. 2002; 119:556–61. [PubMed: 12230495]
32. Wolfman JC, Wolfman A. Endogenous c-N-Ras provides a steady-state anti-apoptotic signal. J Biol Chem. 2000; 275:19315–23. [PubMed: 10777478]
33. Wolfman JC, Palmby T, Der CJ, Wolfman A. Cellular N-Ras promotes cell survival by downregulation of Jun N-terminal protein kinase and p38. Mol Cell Biol. 2002; 22:1589–606. [PubMed: 11839824]
34. Dumaz N, Hayward R, Martin J, Ogilvie L, Hedley D, Curtin JA, et al. In melanoma, RAS mutations are accompanied by switching signaling from BRAF to CRAF and disrupted cyclic AMP signaling. Cancer Res. 2006; 66:9483–91. [PubMed: 17018604]
35. Li Q, Haigis KM, McDaniel A, Harding-Theobald E, Kogan SC, Akagi K, et al. Hematopoiesis and leukemogenesis in mice expressing oncogenic NrasG12D from the endogenous locus. Blood. 2011; 117:2022–32. [PubMed: 21163920]
36. Tsuruma R, Ohbayashi N, Kamitani S, Ikeda O, Sato N, Muromoto R, et al. Physical and functional interactions between STAT3 and KAP1. Oncogene. 2008; 27:3054–9. [PubMed: 18037959]
37. Elad-Sfadia G, Haklai R, Ballan E, Gabius HJ, Kloog Y. Galectin-1 augments Ras activation and diverts Ras signals to Raf-1 at the expense of phosphoinositide 3-kinase. J Biol Chem. 2002; 277:37169–75. [PubMed: 12149263]
38. Elad-Sfadia G, Haklai R, Balan E, Kloog Y. Galectin-3 augments K-Ras activation and triggers a Ras signal that attenuates ERK but not phosphoinositide 3-kinase activity. J Biol Chem. 2004; 279:34922–30. [PubMed: 15205467]
39. Shalom-Feuerstein R, Cooks T, Raz A, Kloog Y. Galectin-3 regulates a molecular switch from N-Ras to K-Ras usage in human breast carcinoma cells. Cancer Res. 2005; 65:7292–300. [PubMed: 16103080]
40. Ahearn IM, Haigis K, Bar-Sagi D, Philips MR. Regulating the regulator: post-translational modification of RAS. Nat Rev Mol Cell Biol. 2011; 13:39–51. [PubMed: 22189424]
41. Barretina J, Caponigro G, Stransky N, Venkatesan K, Margolin AA, Kim S, et al. The Cancer Cell Line Encyclopedia enables predictive modelling of anticancer drug sensitivity. Nature. 2012; 483:603–7. [PubMed: 22460905]
42. Garnett MJ, Edelman EJ, Heidorn SJ, Greenman CD, Dastur A, Lau KW, et al. Systematic identification of genomic markers of drug sensitivity in cancer cells. Nature. 2012; 483:570–5. [PubMed: 22460902]
43. Subramanian A, Tamayo P, Mootha VK, Mukherjee S, Ebert BL, Gillette MA, et al. Gene set enrichment analysis: a knowledge-based approach for interpreting genome-wide expression profiles. Proc Natl Acad Sci USA. 2005; 102:15545–50. [PubMed: 16199517]
44. TCGA. Comprehensive molecular characterization of human colon and rectal cancer. Nature. 2012; 487:330–7. [PubMed: 22810696]

45. Musteanu M, Blaas L, Mair M, Schlederer M, Bilban M, Tauber S, et al. Stat3 is a negative regulator of intestinal tumor progression in Apc(Min) mice. Gastroenterology. 2010; 138:1003–11. e1–5. [PubMed: 19962983]

46. el Marjou F, Janssen KP, Chang BH, Li M, Hindie V, Chan L, et al. Tissue-specific and inducible Cre-mediated recombination in the gut epithelium. Genesis. 2004; 39:186–93. [PubMed: 15282745]

47. Shirasawa S, Furuse M, Yokoyama N, Sasazuki T. Altered growth of human colon cancer cell lines disrupted at activated Ki-ras. Science. 1993; 260:85–8. [PubMed: 8465203]

48. Ventura A, Meissner A, Dillon CP, McManus M, Sharp PA, Van Parijs L, et al. Cre-lox-regulated conditional RNA interference from transgenes. Proc Natl Acad Sci USA. 2004; 101:10380–5. [PubMed: 15240889]

49. Khosravi-Far R, White MA, Westwick JK, Solski PA, Chrzanowska-Wodnicka M, Van Aelst L, et al. Oncogenic Ras activation of Raf/mitogen-activated protein kinase-independent pathways is sufficient to cause tumorigenic transformation. Mol Cell Biol. 1996; 16:3923–33. [PubMed: 8668210]

50. Macdonald JL, Pike LJ. A simplified method for the preparation of detergent-free lipid rafts. J Lipid Res. 2005; 46:1061–7. [PubMed: 15722565]

SIGNIFICANCE

Little is known about N-Ras function in normal biology or in cancer. Our study links the anti-apoptotic function of mutant N-Ras to its ability to promote colorectal cancer in an inflammatory context. In addition, our study pinpoints a therapeutic strategy for this distinct colorectal cancer subtype.

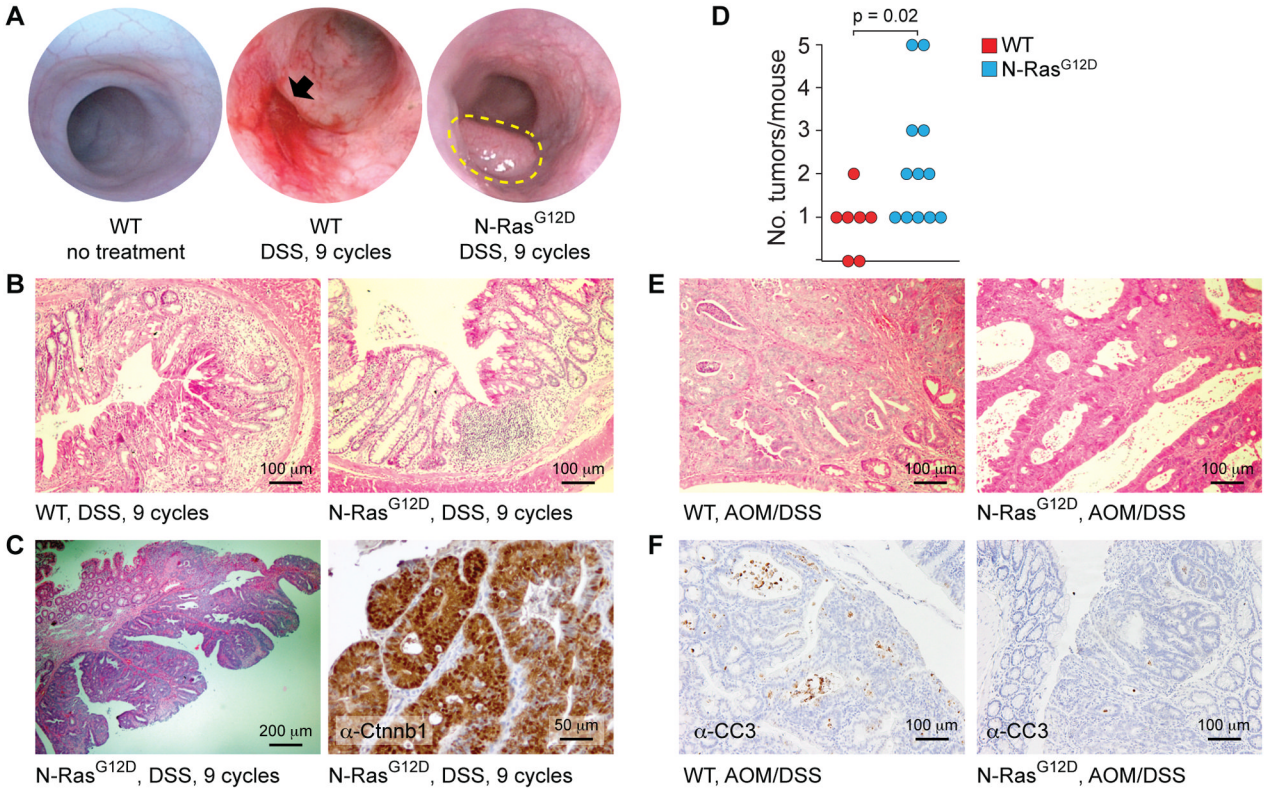

Figure 1.

Mutant N-RAS promotes colon cancer in the context of inflammation. **A.** Colonoscopy images from mice before and after 9 cycles of DSS. WT and N-Ras^{G12D} colons looked identical prior to treatment. After 9 cycles of DSS, WT animals developed severe colitis, which was often associated with bleeding ulcers (black arrow), but never developed tumors. After the same period of time, 50% of N-Ras mutant animals developed colonic tumors (outlined in yellow). **B.** Histologic analysis of tissue damage in WT and N-Ras mutant animals after 9 cycles of DSS. The WT animals exhibited more significant tissue damage. **C.** Histologic analysis of colonic tumors from animals expressing N-Ras^{G12D}. These tumors were adenocarcinomas with high-grade dysplasia. The lesions were strongly positive for nuclear β-catenin (Ctnnb1). **D.** Colonic tumor multiplicities from animals treated with AOM and DSS. WT animals (N = 7) developed, on average, 0.85 tumors per animal, while N-Ras mutant animals (N = 12) developed, on average 2.25 tumors. (p = 0.02, Wilcoxon Rank Sum test). **E.** Histologic analysis of tumors from AOM/DSS treated animals. There was no clear difference between WT and N-Ras mutant tumors. **F.** Immunohistochemical detection of apoptosis in AOM/DSS tumors. Tumors expressing wild-type N-Ras exhibited a greater number of cells positive for cleaved caspase 3 (CC3).

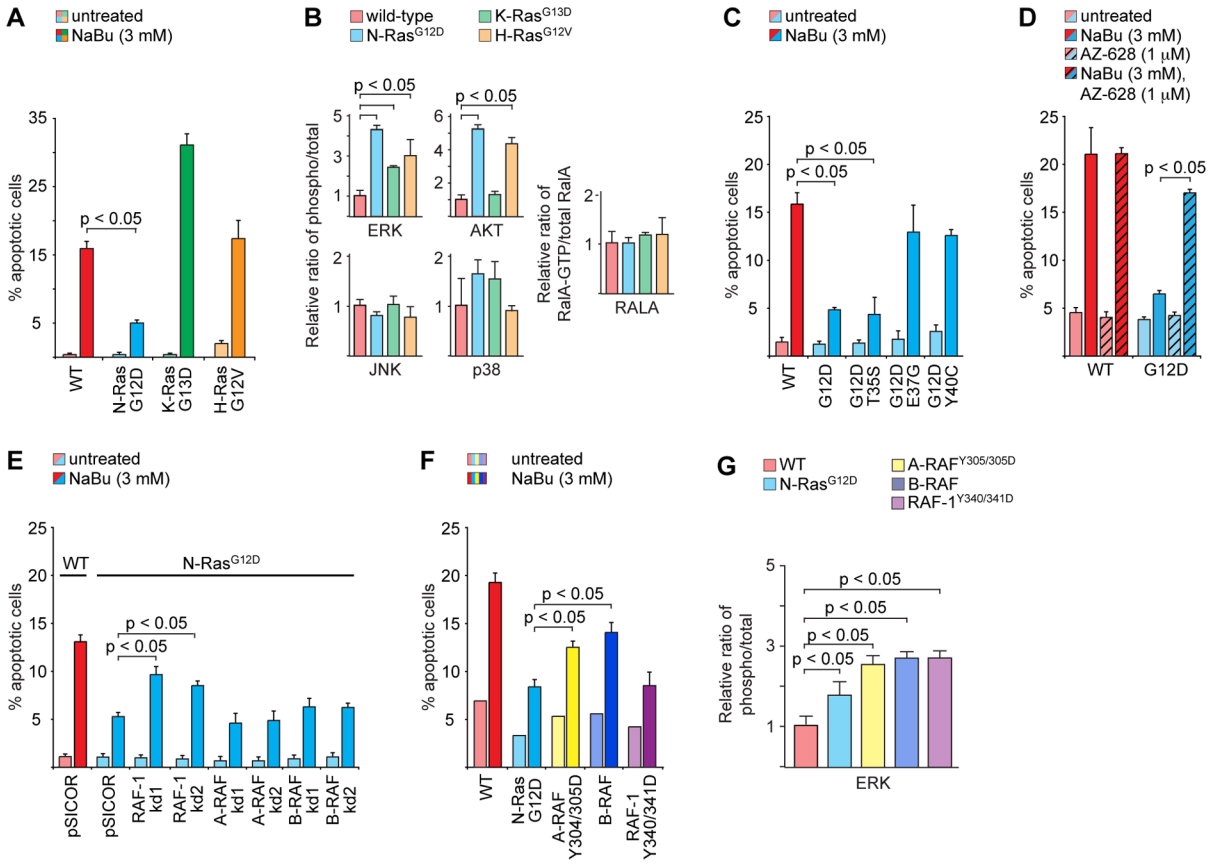

Figure 2.

Mutant N-Ras signals through RAF-1 to confer resistance to apoptosis induced by sodium butyrate. **A.** Apoptotic phenotypes of colon cancer cell lines with mutant forms of Ras. Cells expressing wild-type Ras or H-Ras^{G12V} were sensitive to induction of apoptosis by sodium butyrate (NaBu, 3 mM for 24 hours). Retroviral expression of N-Ras^{G12D} conferred resistance, while endogenous K-Ras^{G13D} conferred hyper-sensitivity. It should be noted that codon 13 mutations in Ras have been shown to elicit attenuated transforming activity when compared to codon 12 mutations. **B.** Canonical effector pathway signaling in cells expressing mutant Ras. Quantitative western blotting revealed that mutant K-Ras, N-Ras, and H-Ras activated ERK, while only N-Ras and H-Ras activated AKT. For ERK, AKT, JNK, and p38, activation was measured as the ratio of phospho to total protein. For RALA, activation was measured as the ratio of GTP-bound protein to total protein. **C.** Apoptotic phenotypes of colon cancer cell lines that express N-Ras^{G12D} secondarily mutated within the effector binding domain. Like N-Ras^{G12D}, N-Ras$^{G12D/T35S}$ conferred resistance to butyrate-induced apoptosis. **D.** Requirement of RAF for the anti-apoptotic phenotype of N-Ras^{G12D}. Treatment of WT cells with AZ-628 did not affect the response to butyrate, but inhibition of RAF in cells expressing N-Ras^{G12D} reverted the anti-apoptotic phenotype. **E.** Effect of RAF knockdown on N-Ras^{G12D} function. Cells expressing N-Ras^{G12D} required RAF-1, but not A-RAF or B-RAF, to fully suppress butyrate-induced apoptosis. **F.** Apoptotic phenotypes of colon cancer cell lines that express mutant forms of RAF. RAF-1$^{Y340/341D}$ fully phenocopied N-RAS^{G12D}. Mutationally activated A-RAF (Y304/305D) and wild-type B-RAF (which has high endogenous kinase activity due to aspartic acid substitutions at the analogous positions) did not suppress butyrate-induced apoptosis. **G.** ERK activation by

mutant RAF. A-RAF, B-RAF, and RAF-1 all activated ERK to the same extent. ERK activation was measured by quantitative western blotting. In all panels, Error bars ± SEM.

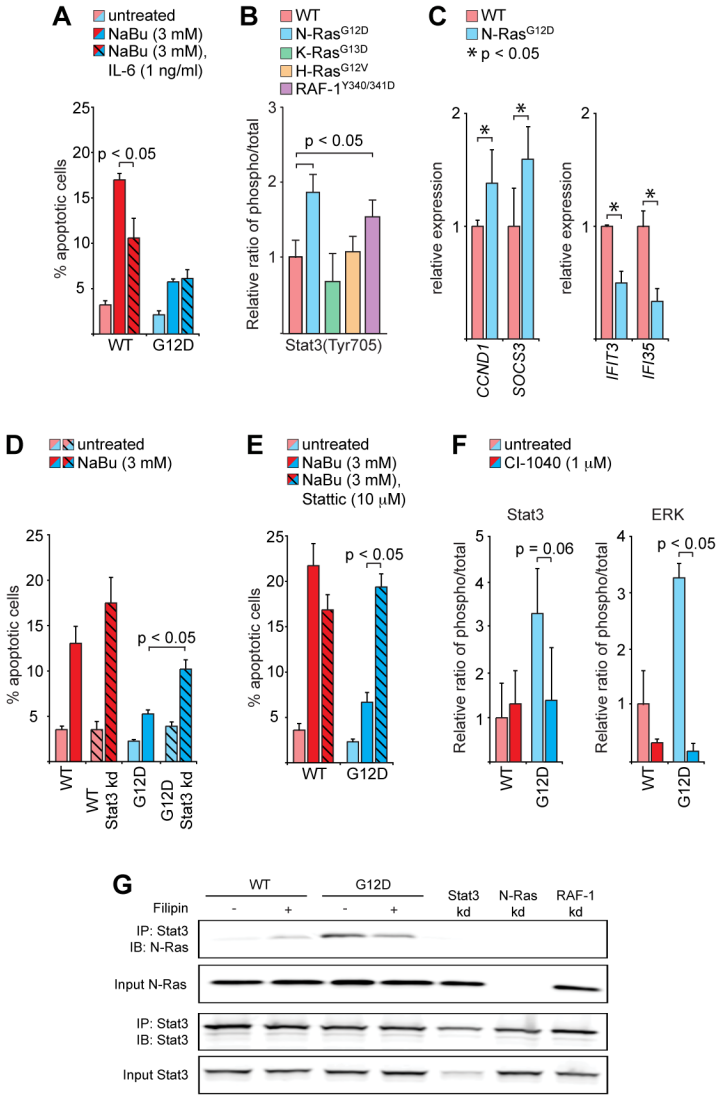

Figure 3.

Mutant N-Ras signals through Stat3 to confer resistance to apoptosis induced by sodium butyrate. **A.** Effect of exogenous IL-6 on butyrate-induced apoptosis. IL-6 significantly suppressed apoptosis in WT cells, but failed to do so in cells expressing N-Ras^{G12D}. **B.** Activation of Stat3 by mutant N-Ras and RAF-1. Expression of N-Ras^{G12D} or RAF-1$^{Y340/341D}$ led to hyper-phosphorylation of Stat3 at a positive regulatory site, Tyr705. Stat3 activation was determined by quantitative western blotting. **C.** Expression of Stat3 target genes. Two genes known to be up-regulated by activated Stat3, *CCND1* and *SOCS3*, were also up-regulated in cells expressing N-Ras^{G12D}. Two genes known to be down-regulated by activated Stat3, *IFIT3* and *IFI35*, were also down-regulated in cells expressing N-Ras^{G12D}. **D.** Effect of Stat3 knockdown on N-Ras^{G12D} anti-apoptotic function. Cells expressing N-Ras^{G12D} required Stat3 to fully suppress butyrate-induced apoptosis. **E.** Effect of Stat3 inhibition on N-Ras^{G12D} anti-apoptotic function. Treatment of WT cells with Stattic, a small molecule Stat3 inhibitor, did not significantly affect the response to butyrate. Inhibition of Stat3 in cells expressing N-Ras^{G12D} reverted the anti-apoptotic phenotype. **F.** Effect of MEK inhibition on Stat3 activation. Treatment with CI-1040 decreased Stat3 phosphorylation on Tyr705 (p = 0.06, Wilcoxon Rank Sum test). The phosphorylation of

ERK was measured as a control for the activity of the MEK inhibitor. **G.** N-Ras interacts with Stat3. α-Stat3 antibody was able to immunoprecipitate both Stat3 and N-Ras in cells expressing N-Ras^{G12D}. This complex was dependent upon the presence of Stat3, N-Ras, and RAF-1. Transient exposure to filipin negatively affected complex formation. In this experiment, in order to control for the overall amount of N-Ras expressed in cells, "WT" denotes cells that ectopically over-express wild-type N-Ras. In panels A–F, Error bars ± SEM.

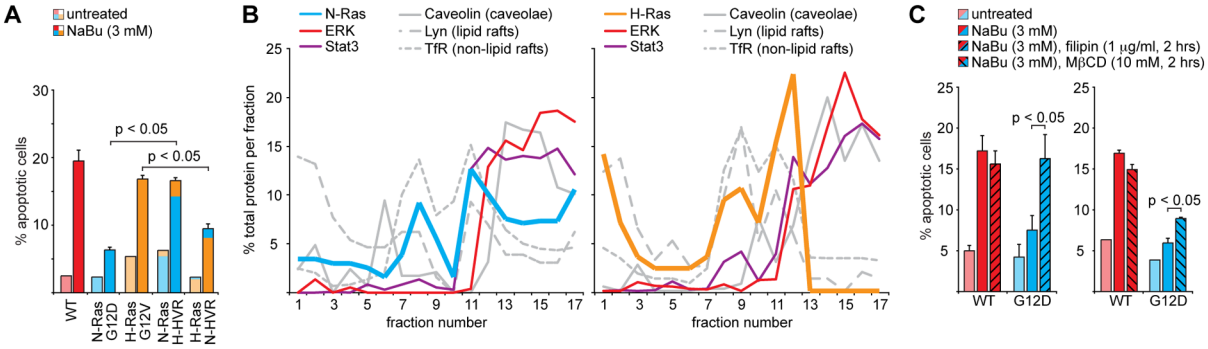

Figure 4.

N-Ras signals from a distinct membrane compartment to suppress apoptosis. **A.** Effects of hypervariable region (HVR) replacement on apoptotic phenotypes of CRC cell lines with mutant forms of Ras. Replacing the N-Ras HVR with that of H-Ras (H-HVR) conferred sensitivity to induction of apoptosis by sodium butyrate. Conversely, replacing the H-Ras HVR with that of N-Ras (N-HVR) conferred resistance to apoptosis. **B.** Biochemical fractionation of plasma membranes. Mutant N-Ras was found primarily in fractions 11–17, while mutant H-Ras was found primarily in fractions 8–12. ERK and Stat3, like N-Ras, were enriched in later fractions. The composition of specific fractions was confirmed by positivity for caveolin, LYN, and/or transferrin receptor (TfR). **C.** N-Ras function requires cholesterol-rich microdomains. Transient treatment with filipin (1 μg/ml for 2 hours) or MβCD (10 mM for 2 hours) abrogated the anti-apoptotic phenotype of mutant N-Ras, but did not affect the response of WT cells to sodium butyrate. In panels A and C, Error bars ± SEM.

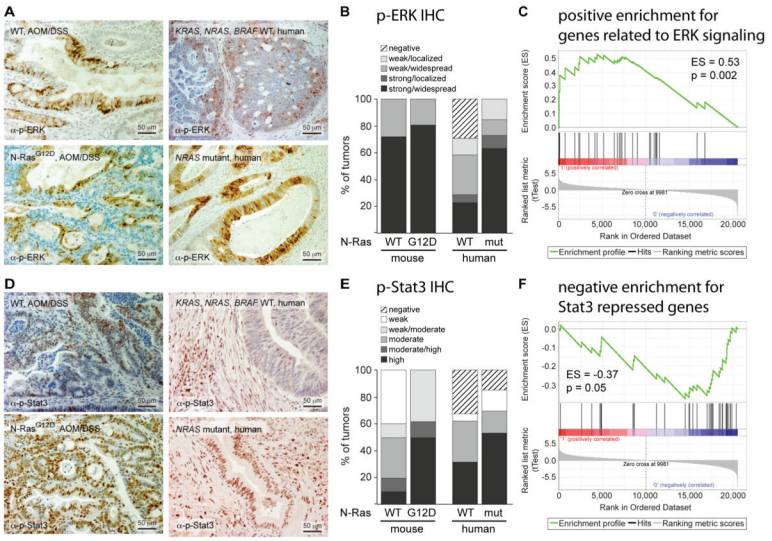

Figure 5.

Activation of ERK and Stat3 in primary tumors expressing mutant N-Ras. **A.** Immunohistochemistry for phospho-ERK in autochthonous mouse and human tumors. **B.** Quantification of phospho-ERK staining in primary tumors. Staining was considerably less variable in mouse tumors. (N = 10 for WT mouse tumors, N = 7 for N-Ras^{G12D} mouse tumors, N = 17 for WT human cancers, N = 19 for *NRAS* mutant human cancers) **C.** Enrichment plot for *NRAS* mutant CRC. Genes related to ERK signaling were significantly enriched in cancers expressing mutant N-Ras. **D.** Immunohistochemistry for phospho-Stat3 in autochthonous mouse and human tumors. **E.** Evaluation of phospho-Stat3 staining in primary colonic tumors from animals treated with AOM/DSS. (N = 10 for WT tumors, N = 8 for N-Ras^{G12D} tumors, N = 17 for WT human cancers, N = 19 for *NRAS* mutant human cancers) **F.** Enrichment plot for *NRAS* mutant CRC. Genes down-regulated by Stat3 were negatively enriched in cancers expressing mutant N-Ras.

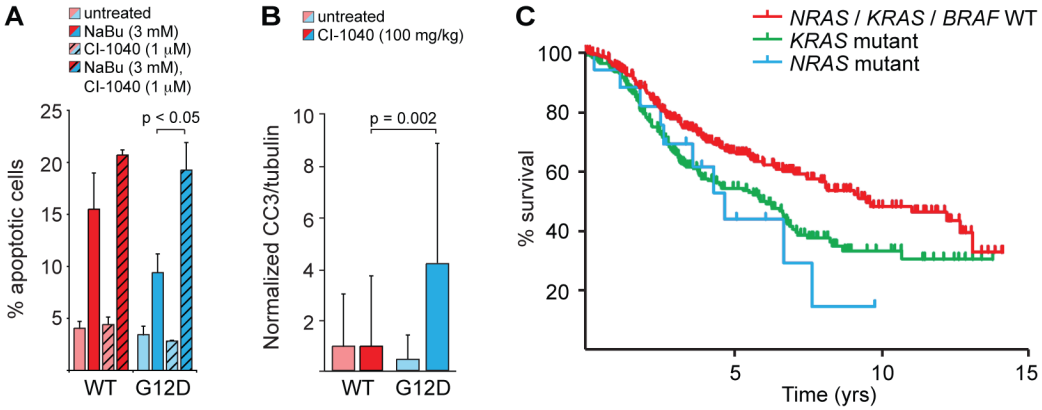

Figure 6.

Inhibition of MEK as a therapeutic strategy for N-Ras mutant CRC. **A.** Requirement of MEK for the anti-apoptotic phenotype of N-Ras^{G12D} in human cell lines. Treatment of WT cells with CI-1040 did not significantly affect the response to butyrate. Inhibition of MEK in cells expressing N-Ras^{G12D} reverted the anti-apoptotic phenotype. **B.** Induction of apoptosis in primary mouse tumors by treatment with CI-1040. Generally, WT tumors did not respond to inhibition of MEK. By contrast, the majority of tumors expressing N-Ras^{G12D} exhibited detectable levels of apoptosis. Apoptosis was detected by quantitative western blotting for cleaved caspase 3 (CC3). (N = 10 for mock-treated WT tumors, N = 9 for treated WT tumors, N = 12 for mock-treated N-Ras mutant tumors, N = 11 for treated N-Ras mutant tumors) **C.** *NRAS* mutation correlates with worse overall survival in CRC patients. Kaplan-Meier plot of overall survival for 314 patients (17 *NRAS* mutant and 297 *NRAS*/*KRAS*/*BRAF* wild-type) with CRC (stages 1–4). The survival of patients with *KRAS* mutant CRC in this cohort is shown for comparison. The difference in survival is statistically significant (p= 0.004, log-rank test). Of the *NRAS* mutant cases, 10/17 were stage 4. For WT cases, 134/297 were stage 4. This difference is not statistically significant (p = 0.3). In panels A and B, Error bars ± SEM.